Commensurability and strong vortex pinning in nanopatterned Nb films

U. Welp,[1] Z. L. Xiao,[1,2] V. Novosad,[1] and V. K. Vlasko-Vlasov[1]
[1]*Materials Science Division, Argonne National Laboratory, Argonne, Illinois 60439, USA*
[2]*Department of Physics, Northern Illinois University, DeKalb, Illinois 60115, USA*
(Received 2 July 2004; revised manuscript received 26 August 2004; published 6 January 2005)

We present a study combining magnetization measurements and direct magneto-optical flux imaging on Nb films, which contain periodic arrays of nanoholes and have been grown on anodized aluminum oxide (AAO) substrates. The magnetization measurements reveal pronounced matching effects in the critical current over the entire temperature range from 4.2 K to T_c. The flux images do not reveal signatures of a domain (terraced) state. Instead, the flux profiles obtained from the images are consistent with the development of a conventional critical state with enhanced vortex pinning. Even though the critical current density in the patterned samples is largely enhanced as compared to the unpatterned reference samples, the self-fields corresponding to the critical state are substantially smaller than the first matching field, H_1. For this reason, a domain state does not appear, and strong pinning arises in a state that is almost commensurate.

DOI: 10.1103/PhysRevB.71.014505 PACS number(s): 74.25.Qt, 74.25.Dp, 74.78.Db

The properties of superconducting vortices in the presence of periodic arrays of pinning centers derive from the interplay between the repulsive elastic vortex-vortex interaction and the attractive vortex-pin interaction. In numerous experimental[1–3] as well as theoretical[4] studies the commensurability effects and the various static and dynamic states arising in such a system have been investigated. In particular, direct vortex imaging[5,6] of carefully prepared field-cooled vortex states has generally confirmed the equilibrium vortex configurations: stable configurations arise in applied fields that correspond to integer multiples or simple fractions of the matching field H_1. At H_1 the number of vortices is equal to the number of pinning sites. However, the vortex behavior under conditions of flux gradient driven dynamics, which is usually encountered in measurements of critical currents and pinning forces, is less well established. The frequent observation of pronounced enhancements of the critical currents, which implies enhanced flux gradients, at multiples of the matching fields is in apparent contradiction to the existence of commensurate states in which the flux density would be uniform. It has been proposed[7,8] that a domain (terrace) state can accommodate macroscopic flux gradients that are associated with flux pinning. Within a domain the flux density is uniform and corresponds to a stable vortex configuration, and the flow of superconducting critical currents is essentially confined to the domain boundaries. This model was used to explain the nonmonotonic field dependence of the magnetization of a Pb film containing a lithographically patterned 1.5-μm-square array of 0.5-μm holes[2] and of a Nb film patterned by a 1.2-μm-square array of 120-nm diameter Ni dots.[3]

Here, we present a study combining magnetization measurements and direct magneto-optical flux imaging on perforated Nb films that have been grown on anodized aluminum oxide (AAO) templates. The films contain a hexagonal pore array with an average pore diameter of 35 nm and a period of 128 nm, corresponding to a matching field of 1459 Oe. Magnetization measurements reveal pronounced matching effects in the critical current over the entire temperature range from 4.2 K to $T_c \approx 7.5$ K, which is in contrast to most lithographically prepared periodic pinning arrays in which matching can be seen only in the close vicinity of T_c. At the lowest temperatures the magnetization displays a nonmonotonic field dependence. The flux images reveal that this nonmonotonic variation is caused by flux avalanches. The flux images do not reveal signatures of a domain (terraced) state at any field. Instead, the flux profiles obtained from the images are consistent with the development of a conventional critical state. Even though the critical current density in the patterned samples is largely enhanced as compared to the unpatterned reference samples, the self-fields corresponding to the critical state are substantially smaller than H_1. For this reason, a domain state does not appear, and strong pinning arises in a state that is almost commensurate.

Anodized aluminum oxide membranes are ideal substrates for fabricating large-area perforated superconducting films with sub-100-nm feature sizes.[9,10] Here we employ a two-step anodization process[11] of high-quality Al foils at 50 V in 0.3*M* oxalic acid to prepare a regular array. The array has perfect hexagonal order with a period of $a = 128$ nm extending over grains of several microns in size.[9–12] This grain size is significantly larger than the superconducting penetration depth, $\lambda \approx 70$ nm (see below). Therefore, the vortex behavior is dominated by the hexagonal periodic pinning array, even though vortices in thin films have long-range interactions [13]. The array period of 128 nm yields a first matching field of $H_1 = \phi_0/[0.5\sqrt{3}a^2] = 1459$ Oe, well in the range of our magneto-optical flux imaging technique. The membrane was covered with a 100-nm film of Nb deposited by magnetron sputtering, followed by a 10-nm-thick Ag capping layer. The average hole diameter in the resulting Nb/AAO film is about 35 nm. Simultaneously with the Nb/AAO samples, continuous reference samples were grown on Si substrates. The critical temperatures of the Nb/AAO films and of the reference films were 7.5 and 7.7 K, respectively. The vortex pinning properties were studied using a SQUID magnetometer, and the distribution of vortices, that is, the normal component of the magnetic induction at the sample surface, was imaged using a magneto-optical technique that utilizes a Bi-doped

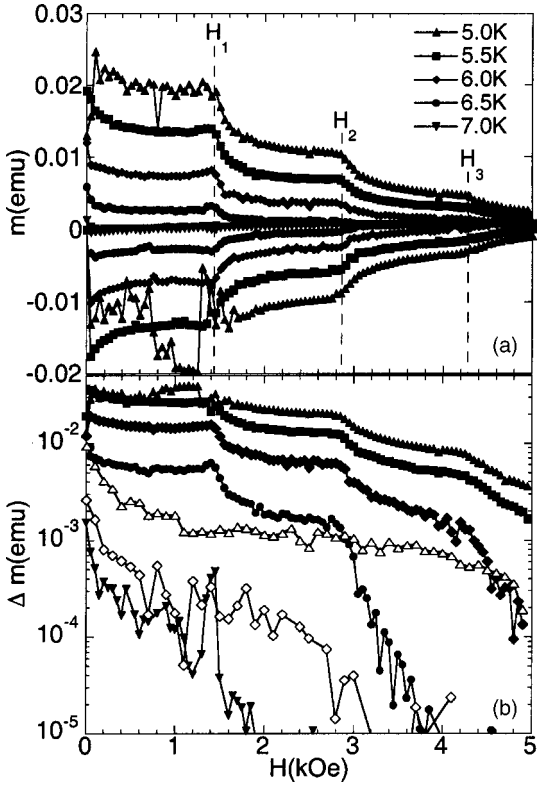

FIG. 1. (a) Field dependence of the magnetic moment of the patterned sample in increasing and decreasing field applied perpendicular to the film at various temperatures. H_1, H_2, and H_3 indicate the location of the first three matching fields. (b) Magnetization hysteresis calculated from the data in the top panel on a logarithmic scale. Included are data for the unpatterned reference sample at 5 K (open triangles) and at 6 K (open diamonds).

garnet layer as optical magnetic field sensor.[14] The garnet layer, with a mirror on one side, is placed directly on the sample, with the mirror side adjacent to the sample. Magnetic stray fields emanating from the sample induce Faraday rotation in the garnet, which is visualized in a polarized light microscope.

The pinning behavior of a rectangular Nb/AAO film with sides $L_1=3.5$ mm and $L_2=2.6$ mm is summarized in Fig. 1. Panel (a) shows magnetization curves $m(H)$ for the field perpendicular to the sample surface taken on sweeping the field up and down after zero field cooling, and panel (b) the corresponding magnetization hysteresis curves, $\Delta m(H)$. The matching field effects appear as steps in the magnetization that become more pronounced at lower temperatures similar to previous observations on a sample with a shorter hole period,[9] but in contrast to the behavior of arrays with micron periods where matching effects disappear just a few tenths of a K below T_c. [1–3] Also included in Fig. 1(b) are the magnetization hysteresis data of a continuous reference sample of the same size as the Nb/AAO sample. Large enhancements of vortex pinning are observed in the Nb/AAO film, which at high fields and temperatures can reach two orders of magnitude as compared to the reference sample. At low temperatures and fields the critical state breaks down through vortex avalanches as evidenced by the nonmonotonic magnetization

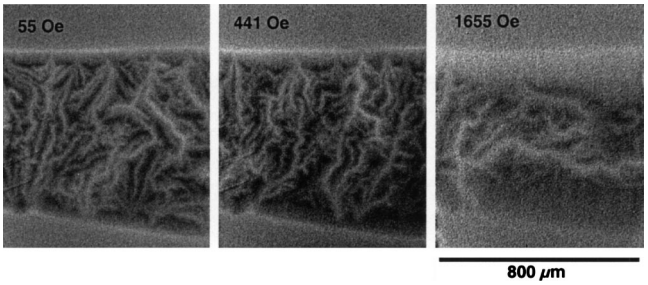

FIG. 2. Magneto-optical images at 5 K for various increasing perpendicular fields showing the evolution of flux avalanches.

curve and discussed in more detail below. Since the magnetization hysteresis between the matching fields is fairly field independent, the critical current density, J_c, can be estimated using the critical state relation for a rectangular sample, $\Delta m = J_c V L_2[1-L_2/3L_1]/2c$. Here, V is the sample volume and $L_1 > L_2$. At 6.0 K and at the first matching field this yields $J_c \approx 1.9\times10^6$ A/cm^2 as compared to 2.0×10^4 A/cm^2 for the reference sample.

Measurements of the upper critical field on these samples[10] indicate a zero-temperature Ginzburg-Landau coherence length and a magnetic penetration depth of $\zeta(0)\approx 10$ nm and $\lambda(0)\approx 70$ nm, respectively. Theoretical estimates[15] show that for the parameters of our samples multiple vortex occupation of a hole does not occur, and that, therefore, the steps at H_2 and H_3 correspond to the nucleation of interstitial vortices. The configuration of the coexisting interstitial and hole-trapped vortices is determined by vortex interaction effects. Since in our high-density hole arrays $\lambda(0)/a > 0.5$, vortex-vortex interactions are strong over the entire temperature range. Thus the interstitial vortices feel a significant cage potential[16] created by the hole-trapped vortices, which explains the strong matching effects even at low temperatures.

The vortex distributions as function of temperature and applied field were imaged on an approximately strip-shaped piece of Nb/AAO with width ~0.8 mm. At low temperatures and sufficiently low fields the critical currents are so high that the critical state becomes unstable towards breakdown through magnetic flux avalanches.[17] They are directly seen in a sequence of magneto-optical flux images shown in Fig. 2. In these images a high vortex density, i.e., a high value of the magnetic induction at the sample surface, is represented by bright contrast. Instead of a smooth, gradual penetration of vortices into the sample, vortices rush into the sample in form of thermomagnetic avalanches that resemble lightning. They occur in a random fashion and, in contrast to the analysis given in previous reports,[2,3] account for the nonmonotonic low-field magnetization of our samples shown in Fig. 1. The images also show that in high fields [Fig. 2(c)] the avalanches give way to smooth flux penetration, consistent with the smooth high-field magnetization curves and the decrease of the critical current density below the threshold value for avalanche formation.[17] We note though that the H-T range for the occurrence of avalanches as seen in the flux images is larger than that in the magnetization measurements. This arises from the more effective cooling of the

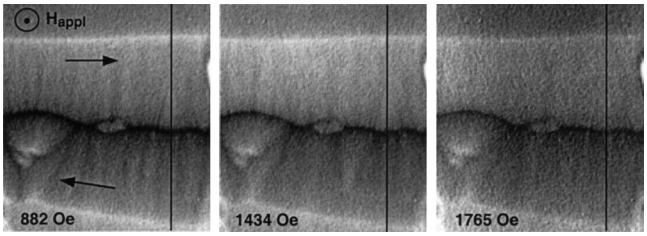

FIG. 3. Magneto-optical images at 6 K for various increasing fields. The bright and dark contrasts at the edges and along the middle of the sample are characteristic features of the fully penetrated critical state. The arrows indicate the flow of the critical currents, and the vertical lines indicate the location of the flux profiles shown in Fig. 4.

sample in magnetization measurements, where the sample is immersed in exchange gas, as compared to optical imaging, where the sample is cooled through thermal conduction via a cold stage.

Figure 3 shows magneto-optical images at 6.0 K on increasing field. The bright contrast along the edges and the dark contrast along the middle are typically observed in a fully penetrated striplike superconducting sample.[14] The irregularities in the flux distribution near the left edge and near the middle of the frame are caused by defects in the sample. Figure 4 shows field profiles taken along the vertical lines in Fig. 3 after subtracting the applied field values. Also included is a fit to the 1434-Oe data according to the model of a superconducting strip in the critical state. In this model in the top half of the strip a constant critical current density, j_c, flows left to right (for an applied field pointing out of the page) and in the bottom half right to left. The distribution of the normal component of the magnetic induction, B_z, generated by these currents is given by Biot-Savart's law:

$$B_z(y,z_0) = \frac{j_c t}{c}\ln\frac{\left(z_0^2+(y-w/2)^2\right)\left(z_0^2+(y+w/2)^2\right)}{\left(z_0^2+y^2\right)^2}.$$

Here, t and w are the thickness and width of the sample, and z_0 is the height above the sample surface at which B is measured. From the width of the peaks at the edge and in the center we estimate $z_0 \approx 20\ \mu$m. This value is largely caused by long-wavelength undulations frequently seen on the surface of AAO membranes. However, since this parameter enters only logarithmically in the above expression an estimate of j_c can nevertheless be obtained. Apart from a slight distortion in the experimental profiles (see below) a fit with $j_c \approx 2.6\times 10^6$ A/cm^2 describes the data reasonably well and this value for j_c is in reasonable agreement with that obtained from the magnetization hysteresis data. The data in Figs. 3 and 4 give no indication for effects due to a geometrical barrier that has been proposed to explain magnetization data on a Nb film patterned with a Ni-dot array.[3] The field dependence of j_c can conveniently be obtained from the difference of the magnetic induction values at the edge in the center, $\Delta B_z = B_z(0) - B_z(w/2) \approx 6(j_c t/c)\ln(w/2\sqrt[3]{2z_0})$. The results closely track the field dependence of Δm, as shown in Fig. 5. The steplike changes occurring at the first matching field are clearly revealed, demonstrating that signatures of the matching effect are contained in the magneto-optical images.

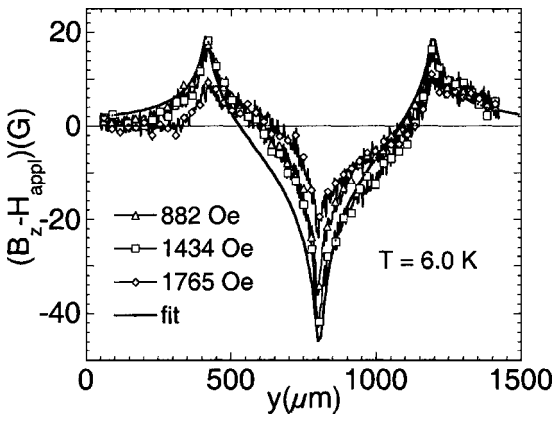

FIG. 4. Flux profiles across the images in Fig. 3 and a fit according to the critical state model.

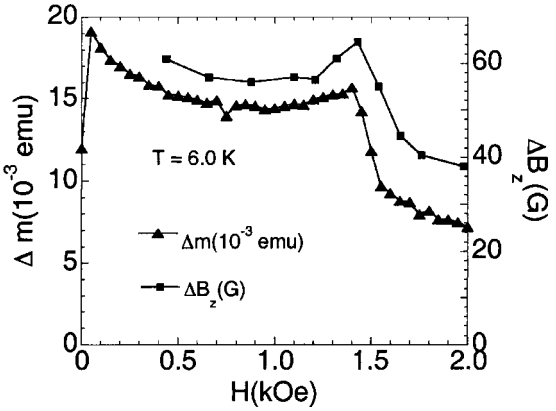

FIG. 5. Comparison of the field dependence of the magnetization hysteresis, Δm, and of the difference ΔB_z of the magnetic induction at the edge and the middle of the sample at 6.0 K.

Over the entire field range covered in Fig. 3 the qualitative picture of the flux distribution does not change. We do not observe signatures of a domain state in which different parts of the sample would have different uniform flux density corresponding to different, stable filling factors.[7,8] Nonuniform vortex rearrangements are visible as bright streaks in Figs. 3(a) and 3(b), which may account for the distorted flux profiles shown in Fig. 4. This type of pattern, which is predominantly oriented perpendicular to the sample edges, arises frequently due to nonuniform vortex nucleation and penetration caused by defect sites at the sample edges.[14,18] In contrast, the domains due to matching effects are expected to be on average oriented parallel to the sample edges in order to accommodate the overall flux gradient. For instance, calculations[8] in the vicinity of the first matching field indicate ribbons of constant vortex density oriented along the sample edges that move towards the sample center on increasing field. For a hexagonal hole lattice it is expected that filling factors[19] of 1, 6/7, 2/3, 1/3, 0 give rise to stable, strongly pinned vortex configurations. We therefore expect that under the experimental conditions of Fig. 3 do-

mains with these filling factors coexist. The difference in vortex density between any of these domains would induce steps in the magnetic induction that is larger than about $1/7\ H_1 \approx 200$ G. Even though the thin-film samples studied here have strongly enhanced pinning, the total variation in the magnetic induction at the sample surface does not exceed about 70 G (see Fig. 5, neglecting effects at the very edge and at the center line), corresponding to roughly $H_1/20$. Therefore, the self-fields of the critical currents are too small to induce a domain state. At the same time, deviations from the ideal commensurate conditions are small. From the data in Fig. 4 one can estimate that the strongest deviations from perfect matching, near the edges and at the center line, would correspond to 1 interstitial and 2 vacancies in every 100 unit cells, respectively. A strongly pinned state can arise due to the over all high stability of the vortex configurations caused by the strong vortex correlations in the vicinity of H_1 as evidenced by the data in Fig. 5. These results therefore suggest that the observation of the domain state necessitates the fabrication of three-dimensional, i.e., thick along the field direction, samples containing nanoscale periodic arrays of linear pinning sites, the sample geometry considered theoretically in Refs. 7 and 8. Large self-fields expected for these samples (for the present sample parameters well above 10 kG) can induce the domain state, and the currents circulating at the domain boundaries can sustain a uniform, perfectly matched B_z (vortex density) inside the domains, in analogy to the uniform field in a long solenoid.

In summary, nanoscale patterned Nb films deposited on AAO substrates display strong enhancements of the critical current density and pronounced matching effects over the entire temperature from 4.2 K to T_c. Magneto-optical flux imaging reveals magnetothermal flux avalanches at low temperatures and fields. No signatures of a domain (terraced) state could be detected in the images. Instead, the observed vortex distributions are consistent with a conventional critical state. We attribute this to the observation that the self-fields of the critical currents are too small to induce a domain state.

This work was supported by the U.S. Department of Energy, Basic Energy Sciences, under Contract No. W-31-109-ENG-38, and by the Consortium for Nanoscale Research at Argonne National Laboratory and the University of Chicago.

[1] A. T. Fiory, A. F. Hebard, and S. Somekh, Appl. Phys. Lett. **32**, 73 (1978); M. Baert, V. V. Metlushko, R. Jonckheere, V. V. Moshchalkov, and Y. Bruynseraede, Phys. Rev. Lett. **74**, 3269 (1995); M. Baert, V. V. Metlushko, R. Jonckheere, V. V. Moshchalkov, and Y. Bruynseraede, Europhys. Lett. **29**, 157 (1995); V. V. Moshchalkov, M. Baert, V. V. Metlushko, E. Rosseel, M. J. Van Bael, K. Temst, R. Jonckheere, and Y. Bruynseraede, Phys. Rev. B **54**, 7385 (1996); *ibid.* **57**, 3615 (1998); E. Rosseel, M. Van Bael, M. Baert, R. Jonckheere, V. V. Moshchalkov, and Y. Bruynseraede, *ibid.* **53**, R2983 (1996); A. Castellanos, R. Woerdenweber, G. Ockenfuss, A. v.d. Hart, and K. Keck, Appl. Phys. Lett. **71**, 962 (1997); T. Puig, E. Rosseel, L. Van Look, M. J. Van Bael, V. V. Moshchalkov, and Y. Bruynseraede, and R. Jonckheere, Phys. Rev. B **58**, 5744 (1998); V. V. Metlushko, L. E. DeLong, M. Baert, E. Rosseel, M. J. Van Bael, K. Temst, V. V. Moshchalkov, and Y. Bruynseraede, Europhys. Lett. **41**, 333 (1998); V. Metlushko, U. Welp, G. W. Crabtree, Z. Zhang, S. R. J. Brueck, B. Ilic, K. Chung, and P. J. Hesketh, Phys. Rev. B **59**, 603 (1999); *ibid.* **60**, R12585 (1999); L. Van Look, E. Rosseel, M. J. Van Bael, K. Temst, V. V. Moshchalkov, and Y. Bruynseraede, *ibid.* **60**, R6998 (1999); J. I. Martin, M. Vélez, J. Nogués, and I. K. Schuller, Phys. Rev. Lett. **79**, 1929 (1997); *ibid.* **83**, 1022 (1999); D. J. Morgan and J. B. Ketterson, *ibid.* **80**, 3614 (1998); Y. Jaccard, J. I. Martin, M.-C. Cyrille, M. Vélez, J. L. Vicent, and I. K. Schuller Phys. Rev. B **58**, 8232 (1998); A. Hoffmann, P. Prieto, and I. K. Schuller, *ibid.* **61**, 6958 (2000); O. M. Stoll, M. I. Montero, J. Guimpel, J. J. Åkerman, and I. K. Schuller, *ibid.* **65**, 104518 (2002); A. V. Silhanek, S. Raedts, M. Lange, and V. V. Moshchalkov, *ibid.* **67**, 064502 (2003).

[2] S. Hébert, L. Van Look, L. Weckhuysen, and V. V. Moshchalkov, Phys. Rev. B **67**, 224510 (2003).

[3] A. Terentiev, D. B. Watkins, L. E. De Long, L. D. Cooley, D. J. Morgan, and J. B. Ketterson, Phys. Rev. B **61**, R9249 (2000).

[4] C. Reichhardt, C. J. Olson, and Franco Nori, Phys. Rev. B **57**, 7937 (1998); C. Reichhardt, G. T. Zimányi, R. T. Scalettar, A. Hoffmann, and I. K. Schuller, *ibid.* **64**, 052503 (2001); C. Reichhardt, C. J. Olson, G. T. Zimányi, and R. T. Scalettar, *ibid.* **64**, 144509 (2001); V. I. Marconi and D. Dominguez, *ibid.* **63**, 174509 (2001); B. Y. Zhu, L. Van Look, V. V. Moshchalkov, B. R. Zhao, and Z. X. Zhao, *ibid.* **64**, 012504 (2001).

[5] K. Harada, O. Kamimura, H. Kasai, T. Matsuda, A. Tonumura, and V. V. Moshchalko, Science **274**, 1167 (1996).

[6] S. B. Field, S. S. James, J. Barentine, V. Metlushko, G. Crabtree, H. Shtrikman, B. Ilic, and S. R.J. Brueck, Phys. Rev. Lett. **88**, 067003 (2002); A. N. Grigorenko, G. D. Howells, S. J. Bending J. Bekaert, M. J. Van Bael, L. Van Look, V. V. Moshchalkov, Y. Bruynseraede, G. Borghs, I. I. Kaya, and R. A. Stradling, Phys. Rev. B **63**, 052504 (2001); Phys. Rev. Lett. **90**, 237001 (2003); D. M. Silevitch, D. H. Reich, C. L. Chien, S. B. Field, H. Shtrikman, J. Appl. Phys. **89**, 7478 (2001).

[7] L. D. Cooley and A. M. Grishin, Phys. Rev. Lett. **74**, 2788 (1995).

[8] C. Reichhardt, J. Groth, C. J. Olson, S. B. Field, and F. Nori, Phys. Rev. B **54**, 16 108 (1996).

[9] U. Welp, Z. L. Xiao, J. S. Jiang, V. K. Vlasko-Vlasov, S. D. Bader, G. W. Crabtree, J. Liang, H. Chik, and J. M. Xu, Phys. Rev. B **66**, 212507 (2002).

[10] U. Welp, Z. L. Xiao, V. K. Vlasko-Vlasov, A. Rydh, W. K. Kwok, V. Novosad, J. S. Jiang, D. Rosenmann, S. D. Bader, and G. W. Crabtree, in Proceedings of the 6th European Conference on Applied Superconductivity, Sorrento, Italy 2003, edited by A. Andreone, G. P. Pepe, R. Cristiano, and G. Masullo (Institute of Physics Publishing, Bristol and Philadelphia, 2003), p. 305.

[11] H. Masuda and H. Fukuda, Science **268**, 1466 (1995); Z. L. Xiao, C. Y. Han, U. Welp, H. H. Wang, V. K. Vlasko-Vlasov, W. K. Kwok, D. J. Miller, R. E. Cook, G. A. Willing, and G. W. Crabtree, Appl. Phys. Lett. **81**, 2869 (2002).

[12] F. Li, L. Zhang, and R. M. Metzger, Chem. Mater. **10**, 2470 (1998).

[13] J. Pearl, Appl. Phys. Lett. **5**, 65 (1964).

[14] L. A. Dorosinskii, M. V. Iindenbom, V. I. Nikitenko, Y. A. Ossipyan, A. A. Polyanskii, and V. K. Vlasko-Vlasov, Physica C **203**, 149 (1992); V. K. Vlasko-Vlasov, G. W. Crabtree, U. Welp, V. I. Nikitenko, in *Physics and Materials Science of Vortex States, Flux Pinning and Dynamics*, edited by R. Kossowsky, S. Bose, V. Pan, Z. Durusoy, NATO Science Series E, Vol. 356, (Kluwer, Dordrecht, 1999), p. 205.

[15] A. I. Buzdin, Phys. Rev. B **47**, 11 416 (1993); A. I. Buzdin and M. Daumens, Physica C **294**, 257 (1998); G. S. Mkrtchyan and V. V. Shmidt, Zh. Eksp. Teor. Fiz. **61**, 367 (1971) [Sov. Phys. JETP **34**, 195 (1972)].

[16] I. B. Khalfin and B. Ya. Shapiro, Physica C **207**, 359 (1993).

[17] P. S. Schwartz and C. P. Bean, J. Appl. Phys. **39**, 4991 (1968); R. G. Mints and A. L. Rakhmanov, Rev. Mod. Phys. **53**, 551 (1981); S. L. Wipf, Cryogenics **31**, 936 (1991); E. R. Nowak O. W. Taylor, L. Liu, H. M. Jaeger, and T. I. Selinder, Phys. Rev. B **55**, 11 702 (1997); V. K. Vlasko-Vlasov, U. Welp, V. Metlushko, and G. W. Crabtree, *ibid.* **69**, 140504 (2004).

[18] Th. Schuster, M. V. Indenbom, M. R. Koblischka, H. Kuhn, and H. Kronmüller, Phys. Rev. B **49**, 3443 (1994).

[19] Ch. Reichhardt and N. Gronbech-Jensen, Phys. Rev. B **63**, 054510 (2001).